energies

MDPI

Article

Comparison of Hydrogen Production Efficiency by *Rhodopseudomonas palustris* MP3 and *Rhodopseudomonas harwoodiae* SP6 Using an Iron Complex as an Enhancement Factor

Fariha Kanwal [1,2,3,4], Arifa Tahir [1], Takuya Tsuzuki [3], David Nisbet [5,6,7,8], Junhong Chen [9] and Angel A. J. Torriero [4,*]

1 Environmental Science Department, Lahore College for Women University, Lahore 42000, Pakistan
2 Department of Microbiology and Molecular Genetics, University of the Punjab, Lahore 54590, Pakistan
3 School of Engineering, Australian National University, Canberra, ACT 2601, Australia
4 School of Life and Environmental Sciences, Faculty of Science Engineering & Built Environment, Deakin University, Burwood, VIC 3125, Australia
5 The Graeme Clark Institute, The University of Melbourne, Melbourne, VIC 3010, Australia
6 Department of Biomedical Engineering, Faculty of Engineering and Information Technology, The University of Melbourne, Melbourne, VIC 3010, Australia
7 Aikenhead Centre for Medical Discovery, St Vincent's Hospital Melbourne, Melbourne, VIC 3065, Australia
8 The Medical School, Faculty of Medicine, Dentistry and Health Science, The University of Melbourne, Melbourne, VIC 3010, Australia
9 Geoscience Australia, Canberra, ACT 2601, Australia
* Correspondence: angel.torriero@deakin.edu.au; Tel.: +61-3-9244-6897

check for updates

Citation: Kanwal, F.; Tahir, A.; Tsuzuki, T.; Nisbet, D.; Chen, J.; Torriero, A.A.J. Comparison of Hydrogen Production Efficiency by *Rhodopseudomonas palustris* MP3 and *Rhodopseudomonas harwoodiae* SP6 Using an Iron Complex as an Enhancement Factor. *Energies* **2023**, *16*, 5018. https://doi.org/10.3390/en16135018

Academic Editors: Dimitrios Sidiras, Konstantina Tsigkou and Panagiota Tsafrakidou

Received: 22 May 2023
Revised: 20 June 2023
Accepted: 27 June 2023
Published: 28 June 2023

Abstract: In the present study, an iron(II)-nanoscale organic complex (Fe-NO) was used as an enhancement factor by two different *Rhodopseudomonas* species of purple non-sulphur bacteria (PNSB) to produce hydrogen (H_2). The Fe-NO complex was synthesised using $FeSO_4{\cdot}7H_2O$ and *Eucalyptus viminalis*—a native Australian plant leaf extract—in a 1:2 and 2:1 concentration ratio. Besides, $FeSO_4{\cdot}7H_2O$ was also used as a source of iron(II) for comparison with the Fe-NO complex. The photo-fermentative bacterial cultures were isolated from a fishpond, and only two strains, MP3 and SP6, were found viable after several attempts of quadrate streaking. After phylogenetic analysis, these strains were designated as *R. palustris* MP3 and *R. harwoodiae* SP6. After comparison with the control, the results showed that the PNSBs manifested an approximately 50% higher H_2 yield when the 1:2 Fe-NO complex was used in the fermentation broth at 10 mg/L concentration, where 10.7 ± 0.54 and 10.0 ± 0.49 mL H_2/L were obtained by *R. palustris* MP3 and *R. harwoodiae* SP6, respectively. The study revealed that the 1:2 Fe-NO complex could be an important material for efficient H_2 production.

Keywords: photo-fermentative bacteria; phyto-fabricated NO-Fe complex; *Rhodopseudomonas palustris* MP3; *Rhodopseudomonas harwoodiae* SP6

1. Introduction

Authenticated energy safety is essential for political, economic and social strength. The rapid increase in population and energy demands has led to an expeditious consumption of fossil fuels, which burn with devastating impacts [1,2]. The continual emissions of greenhouse gases, such as CH_4, CO_2, and N_2O, are responsible for climate change and global warming, which cause glaciers to melt, sea levels to rise and human health to suffer [3], with CO_2 emission constituting 57% of emissions [4]. Considering the effects of climate change, world leaders have united in trying to minimise greenhouse gases and to cut back on average global warming to 2 °C above the preindustrial average world temperatures during the United Nations Climate Change Conference and the Conference of the Parties

in Paris [2]. This has led researchers to focus on developing alternative energy sources that are cost-effective, environmentally friendly and sustainable. In addition to renewable energy sources, biofuels such as biodiesel, bioethanol, biomethane and biohydrogen play an important role [5]. Hydrogen (H_2) has become an eye-catching fuel because it does not emit greenhouse gases. It is called zero-carbon fuel because only H_2O is generated as a waste product. In terms of energy per unit mass, hydrogen is the most efficient energy carrier (142 Kj/g) [6]. It can be produced by various thermochemical (steam reforming of methane, water electrolysis process and biomass gasification) and biological technologies. H_2 gas is employed in multiple sectors, from transportation to electricity generation [3].

The biological routes of H_2 production are biophotolysis, photo-fermentation, dark fermentation and microbial electrolysis cells [2,3,5–8]. According to life cycle assessment and techno-economic studies, dark fermentation is considered the best method for H_2 production [9]. However, photo-fermentation using purple non-sulphur bacteria (PNSB) offers several advantages, including 100% electron release from the organic acids by photosynthetic bacteria, which results in high H_2 yields [2].

Research shows photo-fermentation can enhance H_2 production by implementing various oxide nanoparticles and metal ions [3]. The role of iron is critical in the photo fermentative production of H_2 because it helps in the function of ferredoxin as an electron transporter in the nitrogenase enzyme system [10]. Nitrogenase is found in cyanobacteria, archaea and PNSB. In nitrogen-fixing bacteria, it facilitates the production of ammonia from nitrogen and is also responsible for H_2 generation under nitrogen-deficient conditions [11,12]. Three types of nitrogenases have been found in the microorganisms. These are Fe-nitrogenase, V-nitrogenase and Mo-nitrogenase. All nitrogenases have a similar structure, but compared to Mo-nitrogenase, V and Fe nitrogenases have FeFe and VFe cofactors that boost H_2 generation. Most microorganisms have only Mo-nitrogenase, but *Rhodopseudomonas palustris* has all three types of nitrogenases [13]. However, few studies have used iron nanoparticles synthesised by chemical and ionic methods for H_2 production by photo-fermentation technique [14,15]. Furthermore, no data have been obtained using the Fe-NO complex, which is composed of $FeSO_4{\cdot}7H_2O$ and *Eucalyptus viminalis*—a native Australian plant leaf extract—[6], as an enhancement factor for H_2 production through photo-fermentation by *Rhodopseudomonas palustris* MP3 and *Rhodopseudomonas harwoodiae* SP6.

The current study compares the H_2 production efficiency of *R. palustris* MP3 and *R. harwoodiae* SP6 by Fe-NO complex as an enhancement factor. The PNSB *R. palustris* MP3 and *R. harwoodiae* SP6 were isolated from the native environment of a fishpond and were used in this study due to their adaptably and ability to use different carbon sources to generate H_2 using nitrogenase enzymes [16]. The Fe-NO complex used in the present research was synthesised at two different concentration ratios (1:2 and 2:1). The results for enhanced production of H_2 were compared with that of iron(II) obtained from $FeSO_4{\cdot}7H_2O$ and the control with no iron(II) added.

2. Materials and Methods

Materials: Iron(II) sulphate heptahydrate, sodium hydroxide, sodium succinate (dibasic), sodium acetate, acetone, boric acid, calcium chloride, nickel chloride, manganese sulphate, bovine serum albumin, sodium chloride, potassium dihydrogen phosphate, cobalt chloride, sodium molybdate, ammonium chloride, copper chloride, zinc sulphate, ammonium chloride, magnesium sulphate, cysteine-hydrochloric acid, ethanol, methanol, iron citrate, sodium lactate, potassium oxalate, sodium propionate, yeast extract and agar were purchased from Sigma-Aldrich and used as received. Fe-NO complex was synthesised following previously published procedures [6].

Methods: Water specimens were obtained from the fishpond at the University of the Punjab Lahore, Pakistan, at a 50 cm depth utilising sterile glass bottles. The pond's water temperature and pH levels were gauged with a portable thermometer and a pH meter (WTWpH 340i, Weilheim, Germany).

The PNSBs were isolated following a previously reported procedure [6]. Initially, sterilised Schott bottles were filled with 10 mL of each water specimen, which was then complemented with sterile mineral salt succinate (MSS) media. Next, a precise volume of sterile vegetable oil was introduced to the medium to establish anaerobic conditions conducive to bacterial growth, leaving minimal overhead space. Then, the Schott bottles were placed in an incubator (Memmert Model ICP, Büchenbach, Germany) and exposed to a light intensity of 3000 lux and 30 °C for one week. After this time, sequential dilution of enrichment cultures was performed. Subsequently, three agar plates were prepared for each dilution by transferring 50 µL onto the plates, which were then placed in an anaerobic jar (OXOID AG0025, Basingstoke, UK) at 30 °C and 3000 lux for seven days. Following this period, 30 colonies were selected from all the plates and inoculated onto newly prepared, modified MSS agar plates in a square pattern. After multiple streaking attempts, two strains were successfully purified.

The metabolic responses of individual bacterial species to various carbon substrates were assessed, utilising propionate, citrate, acetate, lactate, oxalate, and succinate, with this last compound serving as a baseline comparison. Moreover, each of these carbon substrates, with a quantity of 1.0 g, was incorporated with other nutrients in the MSS growth medium. Subsequently, the medium was sterilised and inoculated in triplicate with two viable bacterial species. Post-inoculation, the vials were stored in anaerobic, light-exposed conditions at 30 °C for seven days. To evaluate the influence of yeast extract as the sole nitrogen source, different doses (0.6, 0.8, and 1.0 g/L) were implemented without the inclusion of any carbon source. Furthermore, a control sample was prepared using 1.0 g of succinate and 1.0 g of yeast extract.

The isolated bacterial species were sequenced for the 16S rRNA gene using the dideoxy method by Macrogen Inc. (Seoul, Republic of Korea). First, the received sequences were reviewed for base call accuracy and tidied up using Finch TV. Next, contigs were created using the 2-sequence BLAST tool from NCBI. The contigs were then categorised by employing the 16S rRNA database of NCBI BLAST. Finally, the closest homologue sequences were procured and used to construct a neighbour-joining phylogenetic tree using Mega 5.0 [17], with a 100-bootstrap value serving as a verification of the phylogenetic tree [18].

The photo-fermentative experiment was performed in duplicates utilising 100 mL serum vials filled with 60 mL of an altered MSS broth [6,19]. These vials also contained 0.5 g/L-cysteine-HCl. The pH level of the broth was kept within the range of 6.8 to 7.2. The medium was subjected to boiling and then cooled under a nitrogen atmosphere. The prepared medium was then portioned out into the serum vials. Each vial was securely sealed using rubber stoppers and aluminium seals, followed by sterilisation through autoclaving. After autoclaving, the nitrogen atmosphere in the serum vials was displaced with argon gas. Each serum vial was aseptically inoculated with a 10% inoculum. The inoculated vials were incubated at 30 °C and 3000 lux for 5 days.

The hydrogen content in the headspace of each sample vial was measured using gas chromatography (GC, 6890N Agilent Technologies, Santa Clara, CA, USA), which was fitted with an eight-foot molecular sieve 5A 60/80 mesh and three-foot HayeSep Q 80/100 mesh packed columns (Supelco, Sigma-Aldrich, Castle Hill, Australia) in conjunction with a thermal conductivity detector. A certified standard gas mixture containing 0.5 mol% helium and 0.5 mol% H_2 balanced in argon (manufacturer: BOC, Preston, Australia) was employed as a reference. The GC oven and the detector were set at 90 and 150 °C, respectively. High-purity argon was used as the carrier gas. From the vial's headspace, a volume of 1.0 mL of gas was extracted with an airtight glass syringe and subsequently introduced into the GC's injection port. The analytical process spanned 10 min. Three separate measurements were collected for each presented data set to ensure the precision of our results. The final H_2 concentration was reported in ppm. LOQ of H_2 is 2 ppm and analytical variation <0.15%.

The dry cell weight and carotenoid content were assessed following an established protocol [20]. In summary, a 10 mL sample from the fermentative mixture was centrifugated for 30 min at 4000 rpm. Following the removal of the supernatant, the cellular mass was

subjected to three or four rounds of washing using sterile distilled water to eliminate any residual debris from the cells. The centrifuge tubes were then placed in a hot air oven (Memmert, Büchenbach, Germany), set at 105 °C, for 24 h.

To quantify the carotenoid concentration, 3.0 mL of the fermentative specimen was centrifugated for half an hour at 4000 rpm. Subsequently, the supernatant was removed, and the cell mass was washed several times with DI water. Then, a 4.9 mL 7:2 acetone/methanol mixture was added, and the resulting suspension was stored at 4 °C for 30 min. After this period, a second round of centrifugation was conducted on the samples, followed by measuring the Optical Density at 480 nm using a Varian Cary 60 UV-Vis spectrophotometer (Agilent Technologies, Santa Clara, CA, USA).

3. Results

The purple non-sulphur bacteria (PNSB) isolated in this work were readily distinguishable by their reddish colour, a visual trait that becomes prominent when cultured in an anaerobic, illuminated environment, given favourable pH and temperature conditions. Furthermore, physiological assessments verified that these isolated colonies exhibited a Gram-negative reaction and adopted a rod-like shape. Moreover, these specific strains demonstrated the ability to proliferate in a dark, aerobic setting without any pigmentation, utilising organic matter as a nutrient source [21,22].

The availability of carbon and nitrogen sources significantly influences PNSB growth and augments the functionality of the nitrogenase enzyme [23]. The carbon substrates used to promote bacterial proliferation included acetate, citrate, lactate, succinate, oxalate, and propionate, while yeast extract, at varying concentrations, was employed as the exclusive nitrogen source (Table 1). Except for citrate, upon exposure to the different carbon sources, both PNSB strains demonstrated growth. Among these carbon sources, succinate emerged as the most conducive to bacterial proliferation. The optimal concentration of yeast extract, when combined with a carbon source, was established to be 1.0 g.

Table 1. Physiological characterisation of bacterial cultures.

Sr. No.	Strain	Carbon Sources (g/L)						Nitrogen Source = YE (g/L)			
		Propionate	Citrate	Acetate	Oxalate	Lactate	Succinate	C	1.0	0.8	0.6
1	MP3	+++	-	+++	+	+	++++	++++	+++	+++	+
2	SP6	++	-	+	+	+	++++	++++	+++	++	+

++++ = Excellent; +++ = Good; ++ = Medium; + = Low; - = No growth; YE = Yeast Extract, C = Control.

To identify the selected strains, sequencing outcomes were analysed and found to be closely associated with the *Rhodopseudomonas* subgroup. Morphological and physiological characteristics further affirmed the resemblance to the *Rhodopseudomonas* species [24]. Notwithstanding they belong to the *Rhodopseudomonas* subgroup, slight variations were observed at the species level. Strain MP3 bore a resemblance to *R. palustris*; hence it was classified as *R. palustris* MP3. On the other hand, SP6 showed a relation to *R. harwoodiae;* consequently, it was labelled as *R. harwoodiae* SP6 (Figures 1 and 2). The sequences of *R. palustris* MP3 and *R. harwoodiae* SP6 have been registered in the NCBI GenBank under the accession numbers MK850206 and MK850207, respectively.

The H_2 yield produced by *Rhodopseudomonas* sp. at the temperature range of 25–37 °C was initially evaluated (Figure 3A). *R. palustris* MP3 produced 2.25 ± 0.20 mL H_2/L at 25 °C, with the highest H_2 yield (5.29 ± 0.45 mL/L) obtained at 31 °C. As the temperature continued to rise, a decrease in hydrogen production was noted, reaching a minimum yield of 1.71 ± 0.46 mL H_2/L at 37 °C. Similarly, *R. harwoodiae* SP6 generated the highest H_2 yield (3.97 ± 0.02 mL/L) at 31 °C. However, it was lower than with *R. palustris* MP3 (Figure 3A), consistent with previous reports [25–27].

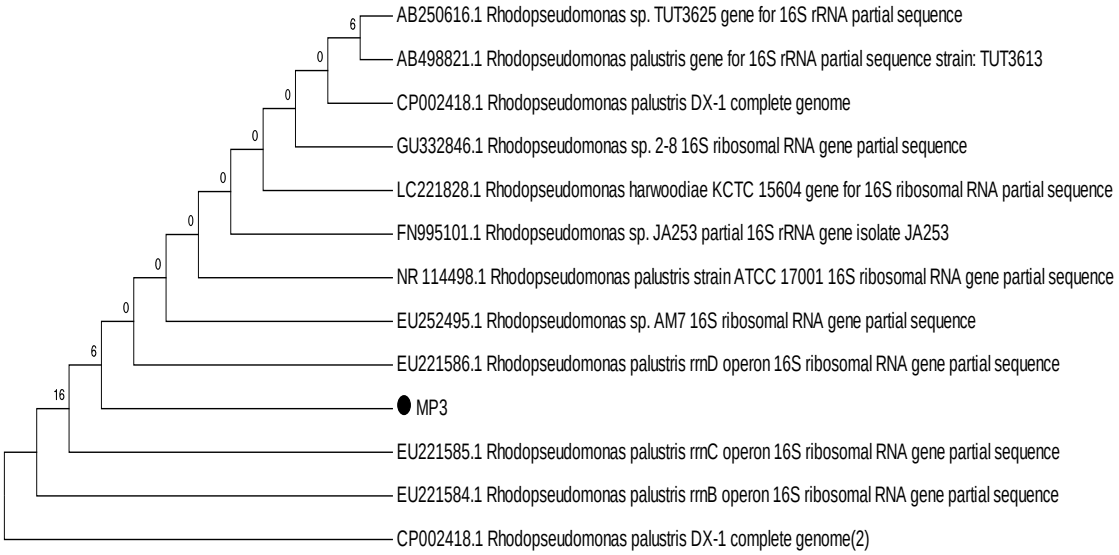

Figure 1. Phylogenetic tree of *Rhodopseudomonas palustris* MP3.

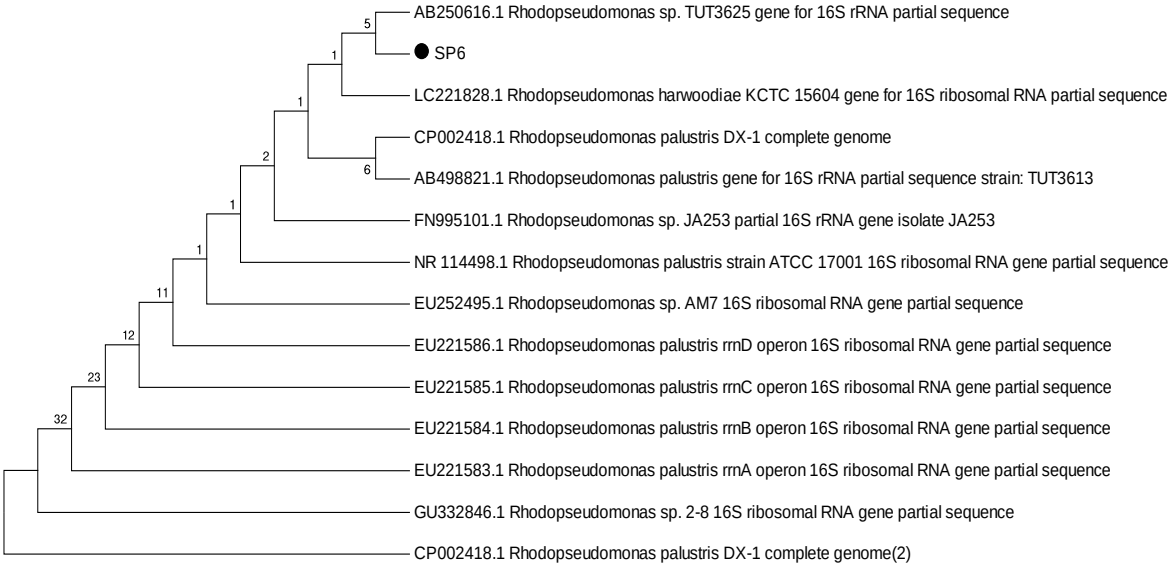

Figure 2. Phylogenetic tree of *Rhodopseudomonas harwoodiae* SP6.

The impact of pH on the H_2 yield by *Rhodopseudomonas* sp. was also investigated (Figure 3B). Different pH values from six to eight were used to observe the effect of iron (II) on enzyme activity for H_2 production. The strain *R. palustris* MP3 produced 2.90 ± 0.32 mL H_2/L at pH 6, which increases up to 5.36 ± 0.42 mL H_2/L when the pH of the system is increased to pH 7. However, elevating the pH value further yielded a decline in H_2 production, reaching a value of 2.30 ± 0.50 mL H_2/L at pH 8. Analogously, the behaviour of *R. harwoodiae* SP6 was also documented, with a maximum volume of 3.83 ± 0.59 mL H_2/L achieved at a pH of 7. These data are congruent with earlier published works on similar bacterial systems [27–31].

The incubation time in the range of 24–168 h on the H_2 yield was evaluated (Figure 3C). *R. palustris* MP3 synthesised 0.82 ± 0.01 mL H_2/L after 24 h of fermentation. It was further increased to 1.94 ± 0.05 mL H_2/L after 48 h of incubation. A gradual increment in the H_2 production up to 5.27 ± 0.35 mL H_2/L was observed after 120 h of incubation, followed by a gradual decline in H_2 production afterwards. Meanwhile, *R. harwoodiae* SP6 generated 3.89 ± 0.18 mL H_2/L following 120 h of fermentation.

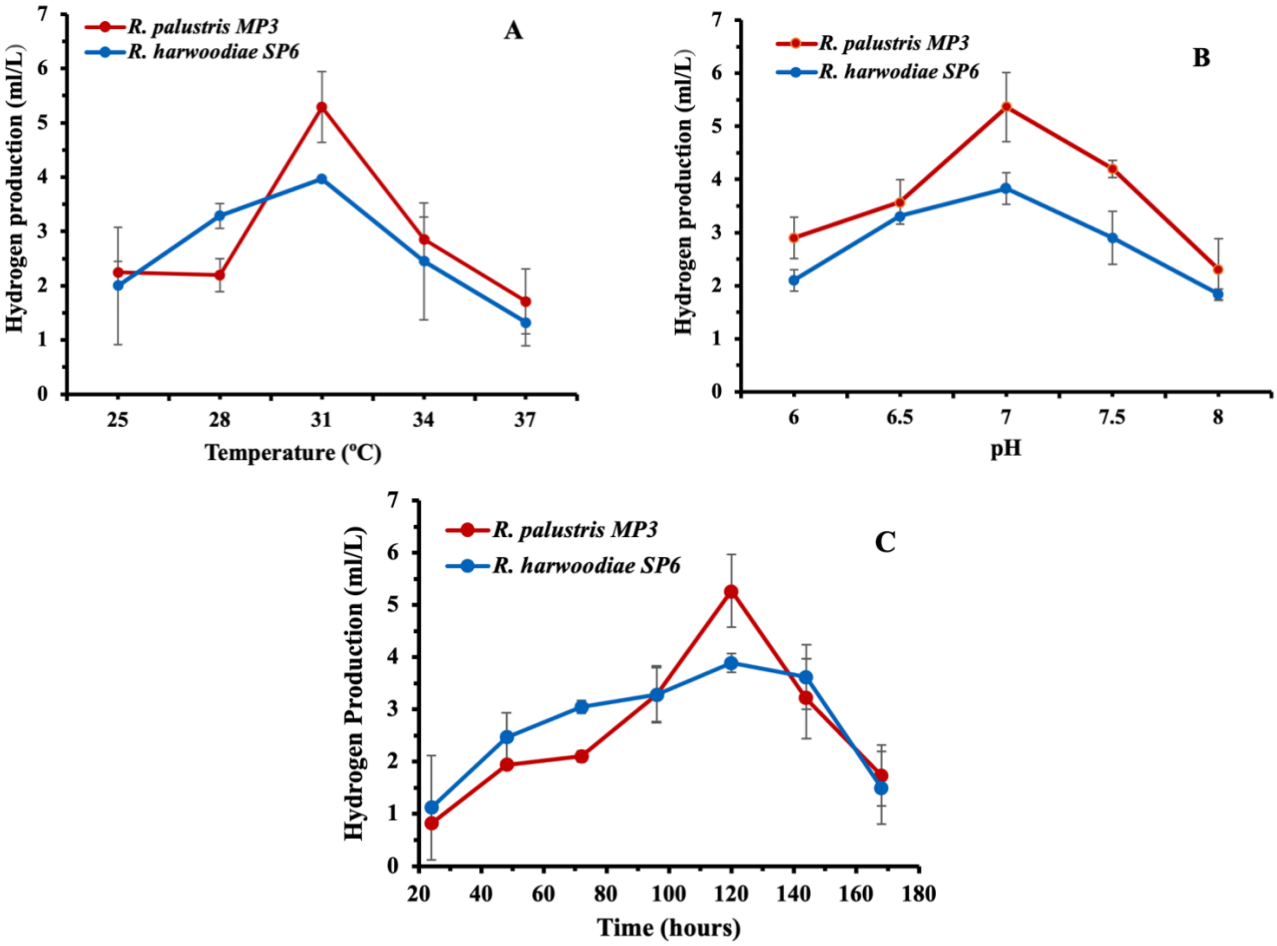

Figure 3. Effect of (**A**) temperature, (**B**) pH and (**C**) incubation time in the production of hydrogen by *Rhodopseudomonas* sp. Error bars = ±SD.

A photo-pigmentation analysis was conducted to ascertain the impact of iron(II) and Fe-NO complex on the photosynthetic system of bacteria. The strains *R. palustris* MP3 and *R. harwoodiae* SP6 both exhibited peaks in the UV-Vis spectrum indicative of chlorophyll a within the 800–900 nm range, as well as carotenoid content in the range 450–600 nm (Figures S1 and S2). No discernible disparities in the spectral ranges were observed when varying concentrations of iron(II) and 1:2 or 2:1 Fe-NO complexes were employed. However, the response of *R. harwoodiae* SP6 deviated from that of *R. palustris* MP3, exhibiting a reduced concentration of cellular mass and pigmentation. The findings suggest that the structural composition of the bacterial photosynthetic system remains unaffected by any form of iron concentration, which agrees with previous observations on related *Rhodopseudomonas* species [6]. Table 2 delineates the influence of iron(II) and 1:2 and 2:1 Fe-NO complexes on the proliferation of bacteria.

Numerous applications of nanoscale organic–iron compounds have been documented, such as green iron nanoparticles, iron–polyphenol complexes, and iron oxide or iron nanoparticles [32–35]. The present study utilised the plant-derived Fe-NO complex and just iron(II) to evaluate H_2 generation by the isolated *Rhodopseudomonas* sp. The *R. palustris* MP3 and *R. harwoodiae* SP6 exhibited differential responses to increasing iron(II) and Fe-NO complexes concentrations within the 0.0–10 mg/L range (Figure 4). Figure 4A demonstrates the influence of iron(II) on H_2 yield and carotenoid synthesis by *R. palustris* MP3. In the absence of iron(II) in the fermentation medium, the H_2 production was 5.29 ± 0.26 mL H_2/L, which increases to 7.85 ± 0.40 mL H_2/L when the iron(II) concentration is 2.5 mg/L. Further increment in the iron(II) concentration up to 10 mg/L produces a decrease in the H_2 yield to 3.55 ± 0.20 mL H_2/L. It is worth noting a strong correlation (r = 0.84) of

H_2 production with the observed levels of carotenoids produced. A similar trend was observed with *R. harwoodiae* SP6 (Figure 4D), where the addition of 2.5 mg/L of iron(II) to the fermentative broth produces an increase in H_2 yield from 3.97 ± 0.19 mL H_2/L (observed in the absence of iron(II)) to 9.64 ± 0.51 mL H_2/L. The H_2 yield decreased to 5.15 ± 0.26 mL H_2/L when 10 mg/L of iron(II) was utilised. This experiment also revealed an r = 0.99 between the H_2 and carotenoid production. The observed increase in H_2 yield could be attributed to the electron carriers and nitrogenase enzymes in photo-fermentative bacteria, which are all iron-containing proteins [15,36]. Meanwhile, the decrease in H_2 production at higher iron(II) concentrations could be attributed to the coagulation effect of iron on the surfaces of bacterial cells [6,15].

Table 2. Optical density showing bacterial growth at different concentrations of $FeSO_4 \cdot 7H_2O$ salt and Fe-NO [a].

Bacterial Strain	Conc. (mg/L)	*R. palustris* MP3	*R. harwoodiae* SP6
Control		1.70 ± 0.04	1.42 ± 0.06
$FeSO_4 \cdot 7H_2O$ salt	2.5	1.81 ± 0.10	1.49 ± 0.30
	5	1.75 ± 0.20	1.49 ± 0.01
	10	1.79 ± 0.03	1.60 ± 0.20
1:2 Fe-NO complex	2.5	1.46 ± 0.20	1.43 ± 0.10
	5	1.81 ± 0.05	1.73 ± 0.02
	10	1.77 ± 0.07	1.42 ± 0.30
2:1 Fe-NO complex	2.5	1.37 ± 0.30	1.29 ± 0.20
	5	1.56 ± 0.10	1.58 ± 0.08
	10	1.71 ± 0.01	1.30 ± 0.40

[a] ± = standard deviation of mean values of replicates (n = 3).

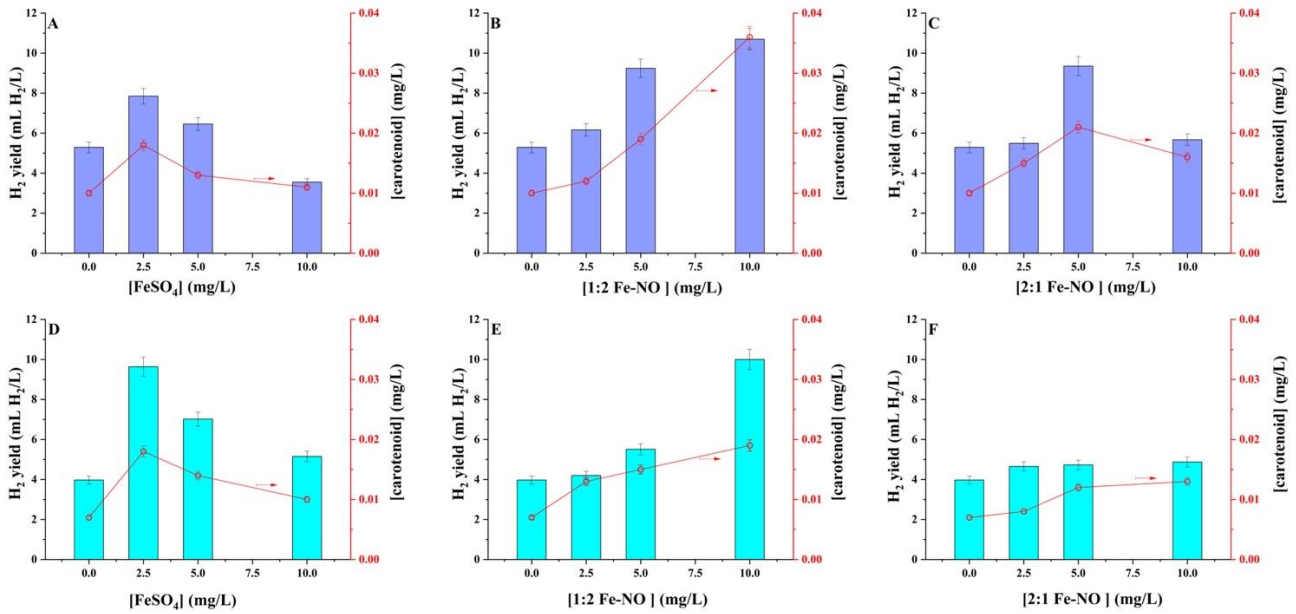

Figure 4. Effect of different concentrations of (**A**,**D**) $FeSO_4$, (**B**,**E**) 1:2 NO-Fe complex and (**C**,**F**) 2:1 NO-Fe complex on H_2 production and carotenoid (○, concentration marked by arrow) by (**A**–**C**) *R. palustris* MP3 and (**D**–**F**) *R. harwoodiae* SP6. Error bars = ±SD.

An enhancement in H_2 production proportional to the concentration of the 1:2 Fe-NO complex was observed for *R. palustris* MP3 and *R. harwoodiae* SP6 strains (Figure 4B,E). When 2.5 mg/L of 1:2 Fe-NO complex was added, the H_2 production by *R. palustris* MP3 reached 6.16 ± 0.31 mL H_2/L, which is approx. 0.91 mL H_2/L larger than the control experiment. The H_2 yield continued increasing with successive additions of the 1:2 Fe-NO complex arriving at a yield of 10.7 ± 0.54 mL H_2/L when a concentration of 10 mg/L

of 1:2 Fe-NO complex was utilised. Notably, the production of carotenoids exhibited a similar pattern to that of H_2 production, showing an r = 0.92 between the H_2 and carotenoid production. The relationship between H_2 and carotenoid production was also consistent in the case of *R. harwoodiae* SP6, where 10 ± 0.49 mL H_2/L and 0.02 ± 0.001 mg carotenoid/mg were obtained when 10 mg/L of 1:2 Fe-NO complex was utilised. However, in this case, no significant difference in H_2 yield is observed when the results of 10 mg/L 1:2 Fe-NO are compared to those obtained with 2.5 mg/L $FeSO_4$, where approx. 10 mL H_2/L is obtained in both cases.

Figure 4C,F depict the effect of the 2:1 Fe-NO complex on H_2 production by *R. palustris* MP3 and *R. harwoodiae* SP6, respectively. An increase in H_2 production to 5.49 ± 0.27 mL H_2/L was observed by *R. palustris* MP3 when 2.5 mg/L 2:1 Fe-NO complex was added. The H_2 yield arrived at the maximum value of 9.35 ± 0.47 mL H_2/L when 5.0 mg/L 2:1 Fe-NO complex was used, with a decrease in H_2 production observed with further addition of 2:1 Fe-NO complex. Figure 4F shows that approx. 4.70 ± 0.20 mL H_2/L was produced by *R. harwoodiae* SP6, independently of the concentration of 2:1 Fe-NO complex used. The production of carotenoids followed a similar trend.

By comparing the results, both strains showed the highest production of hydrogen when the 1:2 Fe-NO complex was used. Overall, *R. palustris* MP3 produced slightly higher volumes of H_2 compared to *R. harwoodiae* SP6. Because the 1:2 Fe-NO complex has doubled the amount of leaf extract than iron(II), PNSB may perform better [6,37]. A study revealed similar results and detected that the iron nanoparticles were advantageous in increasing the production of H_2 as compared to iron(II) salts and control [38,39].

Among the different Rhodopseudomonas species isolated and characterised in our group, *R. palustris* MP3 and *R. harwodiae* SP6 were found to exhibit similar responses to the 1:2 Fe-NO complex as reported for *R. palustris* MP2, which produced 11 mL H_2/L when 10 mg/L of 1:2 NO-Fe complex was used [6]. However, when compared to *R. palustris* MP4, the latter was observed to produce 11 mL H_2/L when 5 mg/L of 2:1 NO-Fe complex was used. Overall, this comparison suggests a potential parity in the impact of iron concentration on hydrogen production, an aspect warranting further exploration.

4. Conclusions

The biostimulation of photo-fermentative bacteria using iron-based nanomaterials enhances the biosynthesis of H_2. In the present work, a complex formed by the combination of the leaf extract of eucalyptus and iron(II) was utilised to evaluate its effect on the production of H_2 by two recently identified strains of *Rhodopseudomonas* sp. It was observed that the Fe-NO complex improved H_2 production by *R. palustris* MP3 and *R. harwoodiae* SP6 compared to iron(II) and control. A yield of 10.7 ± 0.54 mL H_2/L was obtained from *R. palustris* MP3 when 1:2 Fe-NO complex was used at a concentration of 10 mg/L. Using the Fe-NO complex as an H_2 enhancer was an efficient attempt in the field of research. The perspective of future research will focus on investigating the effect of the Fe-NO complex on the activity of nitrogenase enzyme and the recovery of the Fe-NO complex from a fermentation medium for long-term use. There is also a need to investigate the effectiveness of the Fe-NO complex to enhance the yield of hydrogen using various industrial effluents as feedstock.

Supplementary Materials: The following supporting information can be downloaded at: https://www.mdpi.com/article/10.3390/en16135018/s1, Figure S1: UV-Vis spectra showing the effect of $FeSO_4 \cdot 7H_2O$and Fe-NO complex on bacterio-chlorophyll produced by *R. palustris* MP3; Figure S2: UV-Vis spectra showing the effect of $FeSO_4 \cdot 7H_2O$ and Fe-NO complex on bacterio-chlorophyll produced *by R. harwoodiae* SP6.

Author Contributions: F.K. performed all the experimental work and drafted the manuscript. A.T. supervised the overall research. T.T. supervised the preparation and characterisation of the nanoscale organic-iron complex. D.N. helped in experiments related to bio-hydrogen production by PNSB. J.C. helped in the analytical measurements of the bio-hydrogen production by PNSB. A.A.J.T. helped in the conceptualisation, writing, review and editing of the manuscript. All authors have read and agreed to the published version of the manuscript.

Funding: This project was funded by the International Research Support Initiative Program by the Higher Education Commission (HEC) Pakistan, Department of Environmental Science, Lahore College for Women University, Department of Microbiology and Molecular Genetics, University of the Punjab and Research School of Electrical Energy and Materials Engineering, Australian National University.

Data Availability Statement: Data will be made available on request.

Acknowledgments: The authors wish to thank Ziqing Hong (Geoscience Australia) for measuring the H_2 concentration, and Emmanuelle Grosjean and Jacob Sohn (Geoscience Australia) for their thoughtful suggestions during the review process. Junhong Chen publishes with the permission of the CEO of Geoscience Australia.

Conflicts of Interest: The authors declare no conflict of interest.

References

1. Hitam, C.N.C.; Jalil, A.A. A review on biohydrogen production through photo-fermentation of lignocellulosic biomass. *Biomass Convers. Biorefinery* **2023**, *13*, 8465. [CrossRef]
2. Kanwal, F.; Torriero, A.A.J. Biohydrogen&Mdash; A Green Fuel for Sustainable Energy Solutions. *Energies* **2022**, *15*, 7783.
3. Cheng, D.; Ngo, H.H.; Guo, W.; Chang, S.W.; Nguyen, D.D.; Bui, X.T.; Wei, W.; Ni, B.; Varjani, S.; Hoang, N.B. Enhanced photo-fermentative biohydrogen production from biowastes: An overview. *Bioresour. Technol.* **2022**, *357*, 127341. [CrossRef] [PubMed]
4. Yoro, K.; Daramola, M.O. CO_2 emission sources, greenhouse gases, and the global warming effect. In *Advances in Carbon Capture*; Woodhead Publishing: Sawston, UK, 2020; pp. 1–28.
5. Kanmani, S. Enhancement of biological hydrogen production from organic wastes with the application of nanomaterials. *Int. J. Energy Res.* **2022**, *46*, 18929–18946. [CrossRef]
6. Kanwal, F.; Tahir, A.; Qadir Shah, S.A.; Tsuzuki, T.; Nisbet, D.; Chen, J.; Rehman, Y. Effect of phyto-fabricated nanoscale organic-iron complex on photo-fermentative hydrogen production by Rhodopseudomonas palustris MP2 and Rhodopseudomonas palustris MP4. *Biomass Bioenergy* **2020**, *140*, 105667. [CrossRef]
7. Saha, R.; Bhattacharya, D.; Mukhopadhyay, M. Enhanced production of biohydrogen from lignocellulosic feedstocks using microorganisms: A comprehensive review. *Energy Convers. Manag. X* **2022**, *13*, 100153. [CrossRef]
8. Sun, Y.; He, J.; Yang, G.; Sun, G.; Sage, V. A review of the enhancement of bio-hydrogen generation by chemicals addition. *Catalysts* **2019**, *9*, 353. [CrossRef]
9. Hosseinzadeh, A.; Zhou, J.L.; Li, X.; Afsari, M.; Altaee, A. Techno-economic and environmental impact assessment of hydrogen production processes using bio-waste as renewable energy resource. *Renew. Sustain. Energy Rev.* **2022**, *156*, 111991. [CrossRef]
10. Lu, C.; Jiang, D.; Jing, Y.; Zhang, Z.; Liang, X.; Yue, J.; Li, Y.; Zhang, H.; Zhang, Y.; Wang, K.; et al. Enhancing photo-fermentation biohydrogen production from corn stalk by iron ion. *Bioresour. Technol.* **2022**, *345*, 126457. [CrossRef]
11. Khetkorn, W.; Rastogi, R.P.; Incharoensakdi, A.; Lindblad, P.; Madamwar, D.; Pandey, A.; Larroche, C. Microalgal hydrogen production—A review. *Bioresour. Technol.* **2017**, *243*, 1194–1206. [CrossRef]
12. Kim, D.-H.; Kim, M.-S. Hydrogenases for biological hydrogen production. *Bioresour. Technol.* **2011**, *102*, 8423–8431. [CrossRef] [PubMed]
13. Xuan, J.; He, L.; Wen, W.; Feng, Y. Hydrogenase and Nitrogenase: Key Catalysts in Biohydrogen Production. *Molecules* **2023**, *28*, 1392. [CrossRef]
14. Dolly, S.; Pandey, A.; Pandey, B.K.; Gopal, R. Process parameter optimisation and enhancement of photo-biohydrogen production by mixed culture of Rhodobacter sphaeroides NMBL-02 and Escherichia coli NMBL-04 using Fe-nanoparticle. *Int. J. Hydrogen Energy* **2015**, *40*, 16010–16020. [CrossRef]
15. Zhu, H.; Fang, H.H.; Zhang, T.; Beaudette, L.A. Effect of ferrous ion on photo heterotrophic hydrogen production by Rhodobacter sphaeroides. *Int. J. Hydrogen Energy* **2007**, *32*, 4112–4118. [CrossRef]
16. Adessi, A.; Venturi, M.; Candeliere, F.; Galli, V.; Granchi, L.; De Philippis, R. Bread wastes to energy: Sequential lactic and photo-fermentation for hydrogen production. *Int. J. Hydrogen Energy* **2018**, *43*, 9569–9576. [CrossRef]
17. Tamura, K.; Peterson, D.; Peterson, N.; Stecher, G.; Nei, M.; Kumar, S. MEGA5: Molecular evolutionary genetics analysis using maximum likelihood, evolutionary distance, and maximum parsimony methods. *Mol. Biol. Evol.* **2011**, *28*, 2731–2739. [CrossRef] [PubMed]

18. Felsenstein, J. Confidence Limits on Phylogenies: An Approach Using the Bootstrap. *Evolution* **1985**, *39*, 783–791. [CrossRef] [PubMed]
19. Saleem, H.; ul Ain Kokab, Q.; Rehman, Y. Arsenic respiration and detoxification by purple non-sulphur bacteria under anaerobic conditions. *C. R. Biol.* **2019**, *342*, 101–107. [CrossRef]
20. Sawada, H.; Rogers, P.L. Photosynthetic Bacteria in Waste Treatment: Pure Culture Studies with Rhodopseudomonas capsulata. *J. Ferment. Technol.* **1977**, *55*, 297–310.
21. Imhoff, J.F. True marine and halophilic anoxygenic phototrophic bacteria. *Arch. Microbiol.* **2001**, *176*, 243–254. [CrossRef]
22. Karr Elizabeth, A.; Sattley, W.M.; Jung Deborah, O.; Madigan Michael, T.; Achenbach Laurie, A. Remarkable Diversity of Phototrophic Purple Bacteria in a Permanently Frozen Antarctic Lake. *Appl. Environ. Microbiol.* **2003**, *69*, 4910–4914. [CrossRef]
23. Madamvar, D.; Garg, N.; Shah, V. Cyanobacterial hydrogen production World. *World J. Microb. Biot.* **2012**, *16*, 757–767. [CrossRef]
24. Choi, H.-P.; Kang, H.-J.; Seo, H.-C.; Sung, H.-C. Isolation and identification of photosynthetic bacterium useful for wastewater treatment. *J. Microbiol. Biotechnol.* **2002**, *12*, 643–648.
25. Basak, N.; Das, D. Photofermentative hydrogen production using purple non-sulfur bacteria Rhodobacter sphaeroides O.U.001 in an annular photobioreactor: A case study. *Biomass Bioenergy* **2009**, *33*, 911–919. [CrossRef]
26. Lee, K.-S.; Lin, P.-J.; Chang, J.-S. Temperature effects on biohydrogen production in a granular sludge bed induced by activated carbon carriers. *Int. J. Hydrogen Energy* **2006**, *31*, 465–472. [CrossRef]
27. Wang, Y.-Z.; Liao, Q.; Zhu, X.; Li, J.; Lee, D.-J. Effect of culture conditions on the kinetics of hydrogen production by photosynthetic bacteria in batch culture. *Int. J. Hydrogen Energy* **2011**, *36*, 14004–14013. [CrossRef]
28. Cheong, D.-Y.; Hansen, C.L. Feasibility of hydrogen production in thermophilic mixed fermentation by natural anaerobes. *Bioresour. Technol.* **2007**, *98*, 2229–2239. [CrossRef]
29. Fang, H.H.P.; Zhu, H.; Zhang, T. Phototrophic hydrogen production from glucose by pure and co-cultures of Clostridium butyricum and Rhodobacter sphaeroides. *Int. J. Hydrogen Energy* **2006**, *31*, 2223–2230. [CrossRef]
30. Jo, J.H.; Lee, D.S.; Park, D.; Park, J.M. Biological hydrogen production by immobilised cells of Clostridium tyrobutyricum JM1 isolated from a food waste treatment process. *Bioresour. Technol.* **2008**, *99*, 6666–6672. [CrossRef]
31. Nath, K.; Das, D. Effect of light intensity and initial pH during hydrogen production by an integrated dark and photofermentation process. *Int. J. Hydrogen Energy* **2009**, *34*, 7497–7501. [CrossRef]
32. Markova, Z.; Novak, P.; Kaslik, J.; Plachtova, P.; Brazdova, M.; Jancula, D.; Siskova, K.M.; Machala, L.; Marsalek, B.; Zboril, R.; et al. Iron(II,III)–Polyphenol Complex Nanoparticles Derived from Green Tea with Remarkable Ecotoxicological Impact. *ACS Sustain. Chem. Eng.* **2014**, *2*, 1674–1680. [CrossRef]
33. Njagi, E.C.; Huang, H.; Stafford, L.; Genuino, H.; Galindo, H.M.; Collins, J.B.; Hoag, G.E.; Suib, S.L. Biosynthesis of iron and silver nanoparticles at room temperature using aqueous sorghum bran extracts. *Langmuir* **2011**, *27*, 264–271. [CrossRef] [PubMed]
34. Wang, T.; Lin, J.; Chen, Z.; Megharaj, M.; Naidu, R. Green synthesised iron nanoparticles by green tea and eucalyptus leaves extracts used for removal of nitrate in aqueous solution. *J. Clean. Prod.* **2014**, *83*, 413–419. [CrossRef]
35. Wang, Z.; Fang, C.; Mallavarapu, M. Characterisation of Iron–Polyphenol Nanoparticles Synthesised by Three Plant Extracts and Their Fenton Oxidation of Azo Dye. *ACS Sustain. Chem. Eng.* **2014**, *2*, 1022–1025. [CrossRef]
36. Yang, G.; Wang, J. Enhancement of biohydrogen production from grass by ferrous ion and variation of microbial community. *Fuel* **2018**, *233*, 404–411. [CrossRef]
37. Zhou, P.; Elbeshbishy, E.; Nakhla, G. Optimisation of biological hydrogen production for anaerobic co-digestion of food waste and wastewater biosolids. *Bioresour. Technol.* **2013**, *130*, 710–718. [CrossRef]
38. Mohanraj, S.; Anbalagan, K.; Kodhaiyolii, S.; Pugalenthi, V. Comparative evaluation of fermentative hydrogen production using Enterobacter cloacae and mixed culture: Effect of Pd (II) ion and phytogenic palladium nanoparticles. *J. Biotechnol.* **2014**, *192*, 87–95. [CrossRef] [PubMed]
39. Mohanraj, S.; Kodhaiyolii, S.; Rengasamy, M.; Pugalenthi, V. Green synthesised iron oxide nanoparticles effect on fermentative hydrogen production by Clostridium acetobutylicum. *Appl. Biochem. Biotechnol.* **2014**, *173*, 318–331. [CrossRef]